Results in Pharma Sciences 2 (2012) 72–78

Contents lists available at SciVerse ScienceDirect

Results in Pharma Sciences

journal homepage: www.elsevier.com/locate/rinphs

Regenerated keratin membrane to match the *in vitro* drug diffusion through human epidermis

Francesca Selmin[a,*], Francesco Cilurzo[a], Annalisa Aluigi[b], Silvia Franzè[a], Paola Minghetti[a]

[a]*Dipartimento di Scienze Farmaceutiche, Università degli Studi di Milano, via G. Colombo, 71-20133 Milan, Italy*
[b]*CNR-ISMAC, Istituto per lo Studio delle Macromolecole-Corso G. Pella, 16-13900 Biella, Italy*

ARTICLE INFO

Article history:
Received 13 September 2012
Received in revised form 23 September 2012
Accepted 1 October 2012

Keywords:
In vitro skin permeability
Ceramides
Artificial membrane permeability assay
Regenerated keratin

ABSTRACT

This work aimed to develop membranes made of regenerated keratin and ceramides (CERs) to match the barrier property of the human stratum corneum in *in vitro* percutaneous absorption studies. The membrane composition was optimized on the basis of the *in vitro* drug diffusion profiles of ibuprofen, propranolol and testosterone chosen as model drugs on the basis of their different diffusion and solubility properties. The data were compared to those obtained using human epidermis.

The ATR-FTIR and SEM analyses revealed that CERs were suspended into the regenerated keratin matrix, even if a partial solubilization occurred. It resulted in the membranes being physically stable after exposure to aqueous buffer and/or mineral oil and the fluxes of ibuprofen and propranolol from these vehicles through membranes and human skin were of the same order of magnitude. The best relationship with human epidermis data was obtained with 180 μm-thick membrane containing 1% ceramide III and 1% ceramide VI. The data on the testosterone diffusion were affected by the exposure of the membrane to a water/ethanol solution over a prolonged period of time, indicating that such an organic solvent was able to modify the supermolecular organization of keratin and CERs.

The keratin/CER membranes can represent a simplified model to assay the *in vitro* skin permeability study of small molecules.

1. Introduction

Percutaneous absorption is an interdisciplinary topic which is relevant to a number of divergent fields. Indeed, the knowledge of the diffusion of a compound after skin contact is crucial for the evaluation of the risk assessment of toxic substances, the safety of cosmetic ingredients and the design and optimization of pharmaceutical dosage forms as well as medical devices, to be applied onto the skin.

One option to predict the absorption of a compound through the skin by *in vitro* diffusion tests is the use of diffusion cells in which a donor and an acceptor compartment are separated by a suitable membrane [1,2]. Human skin supplied from surgery or cadaver is considered as the "gold-standard" because of the high correlation between *in vitro* and *in vivo* data [3]. Nevertheless, the human skin cannot be readily available and presents large intra- and inter-individual variations up to 45% [4,5]. The quest to circumvent these issues has prompted the research on alternative membranes of mammalian origin. However, differences in stratum corneum thickness, number of corneocyte layers, hair density, water content, lipid profile and morphology cause animal skin to be more permeable than human skin leading to overemphasis of the compound permeability with respect to the human stratum corneum [3,6].

As an alternative, efforts have been made to develop membranes of non-biological origin. Because of the negligible barrier-forming properties of simple polymeric membranes, the comprehension of the role played by the stratum corneum components in the diffusion process is crucial in order to develop predicting *in vitro* assays.

Stratum corneum consists of protein-enriched cells (corneocytes with cornified envelope and cytoskeletal elements) and lipid-enriched intercellular domains. Keratins are major structural proteins in corneocytes forming a cytoplasmic network of 10–12-nm-wide intermediate filaments [7–9]. In particular, intermediate filaments constituting up to 70% of the total dry weight mass of the stratum corneum are coassembles of basic subunits (i.e. type I keratin) and acidic subunits (i.e. type II keratin) having an average molecular weight ranging from 50 to 70 kDa [9]. Moreover, keratins are classified on the basis of the sulphur content which reflects the cross-linking extent and, therefore, its resistance. Due to the low sulphur content, in stratum corneum "soft-keratin" is present. A further classification is based on x-ray diffraction patterns obtained from different keratin proteins. Alpha-helixes appear to be the basis of fibrillar elements in keratins from mammalians [8].

The continuous lipid bilayer is made of various classes of lipids, namely cholesterol, cholesterol esters, free fatty acids, triglycerides and ceramides (CERs), which are arranged in two coexisting lamellar

* Corresponding author. Tel.:+39 02 503 24645; fax: +39 02 503 24657.
E-mail address: francesca.selmin@unimi.it (F. Selmin).

2211-2863/$ - see front matter © 2012 Elsevier B.V. All rights reserved.
http://dx.doi.org/10.1016/j.rinphs.2012.10.001

phases; a long periodicity phase with a repeat distance of about 13 nm and a short periodicity phase with a repeat distance of about 6 nm [10,11]. In particular, CERs have drawn much attention since changes in the CER composition play a role in an impaired skin barrier [12,13]. The various CERs consist of a long-chain sphingoid base linked via an amide bond to a fatty acid and, until now, twelve human CER subclasses have been identified differing in polar head group and chain length [14].

Because of the crucial role of the lipids in the skin barrier function, an *in vitro* model consisting of a porous substrate covered with a layer of synthetic lipids was proposed as a tool to predict solute permeation through human skin [15,16]. A basic lipid model membrane composed of only four constituents was also prepared on porous substrates to study the impact of each CER species on the diffusion and penetration of drugs [17]. To match the permeability of the stratum corneum, synthetic certramides, which are analogues of the ceramides, were selected to develop a skin Parallel Artificial Membrane Permeability Assay (PAMPA) model [18].

The present work aimed to develop a membrane made of a limited number of CERs and keratin which could mimic the barrier property of the human stratum corneum in *in vitro* percutaneous absorption studies. The membrane composition was optimized reducing the number of components in order to simplify its preparation and favour the reproducibility. The membrane performances were tested using three model molecules chosen on the basis of their different diffusion and solubility properties: (RS)-ibuprofen [19], (RS)-propranolol [20] and testosterone [1]. The drug permeation amounts were compared to those obtained in a set of experiments carried out using human epidermis as membrane [1,2].

2. Materials and methods

2.1. Materials

(RS)-Ibuprofen (IB) and testosterone (TS) were obtained from A.C.E.F. (Italy) and Sigma-Aldrich (Italy), respectively. (RS)-Propanolol (PR) was kindly gifted by S.I.M.S. (Italy). Ceramide III, (N-stearyl-D-*erythro*-phytosphingosine) equivalent to human ceramide 3 (CER 3), and ceramide VI, (N-stearyl-2-hydroxy-D-*erythro*-phytosphingosine) equivalent to human ceramide 7 (CER 6), were kindly gifted by Evonik (The Netherlands). All solvents, unless specified, were of analytical grade.

2.2. Keratin extraction

Keratin was extracted from Australian Merino wool, 19.5 μm fineness, by the sulphitolysis reaction, slightly modifying the extraction methods described in previous works [21,22].

Briefly, a fibre sample, withdrawn from a combed sliver and cleaned by Soxhlet extraction with petroleum ether, was washed with distilled water and conditioned at 20 °C, 65% R.H. for 24 h. Five grams of cleaned and conditioned fibres was cut into snippets some millimetres long, put in 100 mL of aqueous solution containing urea (8 M), metabisulphite (0.5 M) and sodium dodecyl-sulphate (SDS), adjusted to pH 6.5 with NaOH 5 N under strong mechanical shaking for 2 h at 65 °C using the Linitest apparatus. The Linitest consists of a water reservoir containing a rotative axle with two stainless steel vessels radially connected. The wool, immersed in the extraction solution, is put in the two vessels with some steel bails and the axle rotates at a frequency of 40 ± 2 rpm. The water temperature is thermostatically controlled and maintained constant during the test.

The mixture was filtered with 5 μm pore-size filter, using a peristaltic pump and dialyzed against distilled water using a cellulose tube (6500 Da molecular cut-off) for 3 days at room temperature, changing distilled water four times a day.

The keratin aqueous solution obtained after dialysis was freeze-dried in order to obtain a keratin powder.

2.3. Membrane preparation

Keratin membranes containing CER3 and CER6 in different ratios (Table 1) were prepared as described below: CER3 and CER6 were dispersed in formic acid using an ultrasound bath at the frequency of 50 Hz for 2 h. Successively, the keratin powder was added to the ceramides dispersion in order to obtain a solution at the keratin concentration of 5% w/w with respect to formic acid. The dissolution of keratin powder was performed under shaking for 2 h at room temperature. Once keratin was dissolved, the solution was subjected to ultrasonic treatment for 2 h in order to remove air bubbles. The solutions were cast in a $5 \times 5\,cm^2$ polyethylene mould at 50 °C until constant weight. The mould was filled with 5, 7, and 10 mL of solution, in order to obtain membranes having a thickness of about 60, or 140, or 180 μm.

2.4. Membrane characterization

The molecular weights of keratin powder were determined by electrophoresis SDS-PAGE. Before electrophoretic analysis, the keratin powder was dissolved in a reductive buffer of dithiothreitol/urea at pH 8.6 under nitrogen atmosphere for 4 h. SDS-PAGE was performed according to Laemmli's method [23] using XcellLock Mini Cell (Invitrogen, USA), on 12% polyacrilamide gels.

The dispersion of the ceramides in the keratin matrix was examined through transmitted light microscopy (DM-LP Transmitted Light Microscope, Leica, Italy).

The surface morphology and the cross sections of the membranes obtained by fracture in liquid nitrogen were investigated by a LEO 435 VP scanning electron microscope (SEM) using an acceleration voltage of 15 kV, a current probe of 400 pA and a working distance of about 24 mm. Samples were sputter-coated with a gold layer 20–30 nm thick in rarefied argon, using an Emitech K550 sputter coater with a current of 20 mA for 240 s.

The thickness of the membranes was measured with a micrometer (MI 1000 micrometer, ChemInstruments, USA).

FTIR measurements were performed using a Spectrum™One spectrophotometer (Perkin–Elmer, USA) by placing the keratin membranes on a diamond crystal mounted on the ATR cell (Perkin–Elmer, USA). The spectra recorded at $4\,cm^{-1}$ resolution and 64 scans were collected over the wavenumber region 4000–650 cm^{-1}. Afterwards, the spectra were elaborated by ATR correction, and automatic baseline corrected and smoothed with a nine-point Savitsky−Golay function [24]. The resultant spectra upon second-derivative analysis yielded the band maxima. Fourier self-deconvolution (FSD) of the amide I band components (1705–1578 cm^{-1}) was performed by using Peakfit 4.12 software (Galactic Industries Corporation, New Hampshire, USA). The amide I bands were resolved by the second-order derivative with respect to the wavelength. Deconvolution was performed using Gaussian line shape with an amplitude threshold of 3%. A nonlinear least-squares method was finally used to take the reconstituted curves as close as possible to the original deconvoluted spectra. The fitting results were further evaluated by examining the residual from the difference between the fitted curve and the original curve and accepted when R^2 was higher than 0.9900. The spectrum of human epidermis was taken as a reference.

2.5. In vitro permeation studies

The skin used in the permeation studies was obtained from the abdominal skin of three donors, who underwent cosmetic surgery (30–50 years old, Eurasian females). Skin samples were prepared following the internal standard procedure [20]. The full-thickness skin

Table 1
Fluxes (μg x h/cm^2) of ibuprofen (IB), propranolol (PR) and testosterone (TS) through keratin membranes at different compositions and thicknesses.

Membrane	Components (%, w/w)			Thickness (μm)	Vehicle	IB		PR	TS
	RK	CER3	CER6			Flux	FoD	Flux	Flux
1	100	–	–	180	Water	9.26 ± 0.04	2.51	–	–
2	99	1.0	–	180	Water	0.34 ± 0.00	0.09	–	–
3	99	–	1.0	180	Water	1.20 ± 0.34	0.32	–	–
4	99	0.5	0.5	180	Water	4.15 ± 0.15	1.13	–	–
5	98	1.0	1.0	180	Water	2.97 ± 0.12	0.80	–	–
					Physiologic solution	–	–	10.0 ± 1.0	–
					Mineral oil	–	–	8.7 ± 3.0	–
					Water/ethanol	–	–	–	7.6 ± 1.7
				140	Water	4.05 ± 0.08	1.10	–	–
				60	Water	6.40 ± 1.59	1.73	–	–
Human epidermis					Water	3.69 ± 1.69*	–	–	–
					Physiologic solution	–	–	17.9 ± 4.3**	–
					Mineral oil	–	–	17.2 ± 5.9**	–
					Water/ethanol	–	–	–	3.8 ± 0.8

* $n = 12$, three donors (Cilurzo et al., 2010a)
** $n = 6$, two donors.

was sealed in evacuated plastic bags and frozen at −20 °C within 24 h after removal.

Prior to experiments, the skin was thawed at room temperature, and the excess of fat was carefully removed. The skin sections were cut into squares of about 2.5 cm^2 and, after immersing the skin in water at 60 °C for 1 min, the epidermis was gently separated from the remaining tissue with forceps and carefully inspected by light microscopy for any defects. Keratin membranes punched out at the area of 2.5 cm^2 were hydrated in MilliQ® water for 1 h.

Afterwards, epidermis or membranes were mounted on the Franz diffusion cell, the receptor compartment of which was filled with a mixture of water/ethanol at the ratio 1:1 for TS [25], pH 7.4 PBS for IB [19] and physiological solution for PR [20]. Special care was taken to avoid air bubbles between the buffer and the epidermis in the receptor compartment.

The upper and lower parts of the Franz cell were sealed with Parafilm® and fastened together by means of a clamp, with the epidermis or membranes acting as seal between the donor and receptor compartments. Then, the donor compartment was filled by an IB saturated solution in MilliQ® water (0.5 mL), or 1 mL PR saturated solution in MilliQ® water (1 mL) and mineral oil (1 mL), or 4 mg/mL TS in water/ethanol at the ratio 1:1 (0.5 mL) and closed. The system was kept at 37 ± 1 °C by means of a circulating water bath so that the epidermis surface temperature was at 32 ± 1 °C throughout the experiment.

At predetermined times (1, 2, 4, 6, 24 h) aliquots of 0.2 mL were withdrawn from the receiver compartment and immediately replaced with fresh receiver medium. The samples were directly assayed by HPLC to determine the drug concentrations. All values represent the averages of parallel experiments performed in triplicate.

The cumulative amount permeated through the skin per unit area was calculated from the concentration of each substance in the receiving medium and plotted as a function of time. The steady flux (J) was determined as the slope of the linear portion of the plot.

To avoid experimental errors due to inter-individual variability, the drug ability to permeate human skin epidermis was evaluated using epidermis sheets from a single donor.

2.6. HPLC methods

The drug concentration was determined by HPLC assay (HP 1100, Chemstations, Agilent Technologies, USA).

RS-Ibuprofen: injection volume: 20 μL; flow rate: 1.5 mL/min; UV absorbance: 225 nm; column: C18 reverse-phase column C18 Nova-Pak, 4.6 × 150 mm^2 (Waters, USA); mobile phase: acetonitrile:water acidified by phosphoric acid at pH 2.6 at the ratio 60:40 (%, v:v); temperature: 25 °C [26].

A standard calibration curve (1–50 μg/mL) was used. The limit of quantification was 0.2 μg/mL.

RS-Propranolol: injection volume: 20 μL; flow rate: 1.0 mL/min; UV absorbance: 225 nm; column: C18 reverse-phase Bondclone, 10 μm, 3.9 × 300 mm^2 (Phenomenex, USA); mobile phase: acetonitrile/0.2% phosphoric acid at the ratio 30:70 (%, v:v); temperature: 25 °C [20].

Three standard calibration curves (0.005–5 μg/mL; 1–40 μg/mL; 10–200 μg/mL) were used. The limit of quantification was 0.004 μg/mL.

Testosterone: injection volume: 50 μL; flow rate: 1.2 mL/min; UV absorbance: 259 nm; column: C18 reverse-phase LiChrospher® 100 100/RP-18, 5 μm, 125 × 4 mm^2 (CPS Analitica, Italy); mobile phase: methanol/water at the ratio 70:30 (%, v:v); temperature: 30 °C.

A standard calibration curve (0.05–51 μg/mL) was used [27].

2.7. Statistical analysis

Tests for significant differences between means were performed by one way-ANOVA. Multiple comparison tests were carried out with Bonferroni–Holm's test. Differences were considered significant at the $p<0.05$ level.

3. Results and discussion

3.1. Regenerated keratin and membrane

Keratin extraction may take place only after cleavage of disulphide bonds and this can be achieved by oxidation, reduction or sulphitolysis [28]. Sulphitolysis describes the cleavage of a disulphide by sulphite to give a thiol and an S-sulphonate anion (or Bunte salt)

$$\mathbf{RSSR} + \mathbf{SO_3^{2-}} \leftrightarrow \mathbf{RS^-} + \mathbf{RSSO_3^-}$$

By introducing in the extraction process a vigorous mechanical shaking through the use of the Linitest apparatus, the keratin extraction yield increases to 40% of the original wool weight. In order to evaluate if the mechanical shaking induces protein degradation, the molecular weight distribution of keratin, extracted as previously described, was determined by electrophoresis SDS-PAGE. The electrophoretic pattern of keratin powder (Fig. 1, line 1) shows the typical molecular mass bands of wool: the two high molecular mass bands at 55 and 45 kDa, related to the low sulphur keratin and the low molecular mass bands between 20 and 9 kDa related to the high sulphur keratin. Therefore, the vigorous mechanical shaking does not degrade the protein. The preparation of pure keratin membranes from formic acid

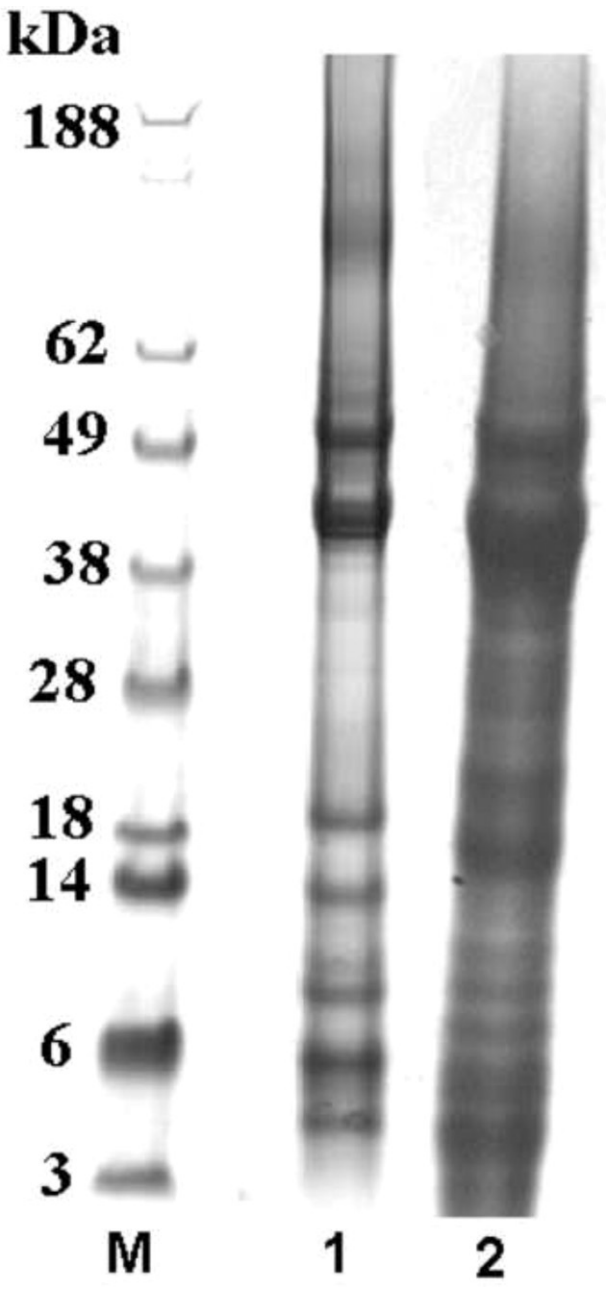

Fig. 1. SDS-PAGE; marker (line M), keratin powder (line 1), and keratin after casting from formic acid solutions (line 2).

solutions was widely studied in a previous work [21]. Despite being a good solvent for keratin, formic acid is also very aggressive and tends to degrade the protein in few weeks. Therefore, after casting of the solutions containing CERs the molecular weights of keratin were controlled (Fig. 1, line 2), in order to test if the combination of formic acid and ultrasonic treatment introduced to remove air bubbles (whose formation is promoted by the CERs presence) degrades the protein. As can be seen in Fig. 1, line 2, only a negligible degradation of the protein occurred.

Keratin membranes containing CER3 and CER6 in different ratios were visually transparent with a smooth and homogeneous surface. As an example, the morphology of Membrane 5 is reported in Fig. 2a. It can be observed that CERs were homogeneously dispersed in the keratin matrix. Moreover, the fractured section (Fig. 2b) shows the ceramide particles embedded in the keratin matrix and pores of about 1 μm. The presence of these pores, previously occupied by CERs, suggests poor adhesion between CERs and keratin.

The supermolecular structure of regenerated keratin and the organization of CERs in the membranes were studied by ATR-FTIR spectroscopy. The ATR-FTIR spectrum of human epidermis was taken as a reference in order to compare the lipid organization in the artificial membranes.

As depicted in Fig. 3, the most relevant bands of stratum corneum are related to the N–H stretching vibration giving rise to the amide A band and the O–H stretching of lipids in the range 3200–3300 cm^{-1}; the CH_3 and CH_2 symmetric and asymmetric vibrations at 2920 and 2850 cm^{-1}, respectively; the lipid ester carbonyl stretching at 1740 cm^{-1}; the C═O and N–H stretching of amide I and amide II at 1650 and 1550 cm^{-1}, respectively; and the CH_X scissoring of lipids backbone at 1470 cm^{-1}. The spectrum of Membrane 1 (Fig. 3) shows the characteristic adsorption bands of regenerated keratin, assigned mainly to the peptide bonds (–CONH–). The amide A band (3282 cm^{-1}) is connected with the stretching vibration of N–H bonds; the amide I band occurring in the 1700–1600 cm^{-1} region is connected mainly with the C═O stretching vibration; the amide II (1520 cm^{-1}) is related to the N–H bending and C–H stretching vibration and, finally, the amide III band occurs in the range of 1220–1300 cm^{-1} and it results from in phase combination of C–N stretching and N–H plane bending vibrations. The intense peaks at 1195 and 1025 cm^{-1} are due to the asymmetric and symmetric stretching vibrations of the Bunte salts residues, respectively. Finally, the bands in the 2950–2850 cm^{-1} region were due to the CH_3 and CH_2 asymmetric and symmetric vibrations.

The spectra of the composite membranes substantially overlapped the keratin sample (Membrane 1), with the exception of the CH_3 and CH_2 asymmetric and symmetric vibrations (Fig. 3). The shift of these bands can be mainly due to the sum of contributes of both CERs and keratin stretching vibrations. Other signals attributed to the presence of CERs in membranes at different compositions were not clearly detected, probably because of the low content.

Since Amide I band mainly reflects the C═O stretching vibration of both CERs and keratins, the deconvolution permits to evidence the hidden peaks determining the single contributes to the spectra and, therefore, the similarity to human epidermis. The deconvoluted amide I spectra in terms of wavenumbers and assignments are reported in Table 2 with reference to literature [29]. In the case of the human epidermis sheets, 11 peak frequencies were identified in FSD spectra. The band centered at about 1633 cm^{-1} was attributed to the intramolecular β-sheet; the peak at 1699 cm^{-1} and the bands in the 1613–1625 cm^{-1} region are due to intermolecular β-sheets. By deconvoluting the region between 1667 and 1694 cm^{-1}, four bands were revealed and assigned to various types of turn structures, which represent the less ordered structure. The contribution of the random coil conformation was identified as two peaks centered at about 1650 cm^{-1}. The band assigned to α-helix was centered at 1659–1660 cm^{-1}. The absorption peak at 1595 cm^{-1} was attributed to the Hys-ring vibration or, more in general, to the keratin side chains. The bands of the keratin membrane (Membrane 1, Table 2) were consistent to those of human epidermis, with the exception of the peaks assigned to CERs which were obviously absent. Two membranes were obtained by using a single CER, and an additional band at 1614 cm^{-1} or 1612 cm^{-1} was revealed (Membranes 2 and 3, Table 2). The peak frequencies were close to those of the commercial ceramides (CER3: 1611 cm^{-1}; CER6: 1617 cm^{-1}). In the deconvoluted spectra of membranes prepared with both CERs, one or two peaks were detected at 1611 cm^{-1} and 1618 cm^{-1} with respect to the concentration of the lipophilic compounds within the membranes (Membranes 4 and 5, Table 2). The lack of the band attributed to CER6 in the spectrum of Membrane 3 was attributed to the different intensity of the amide I band in the commercial samples of CER3 and CER6, the latter being significantly lower.

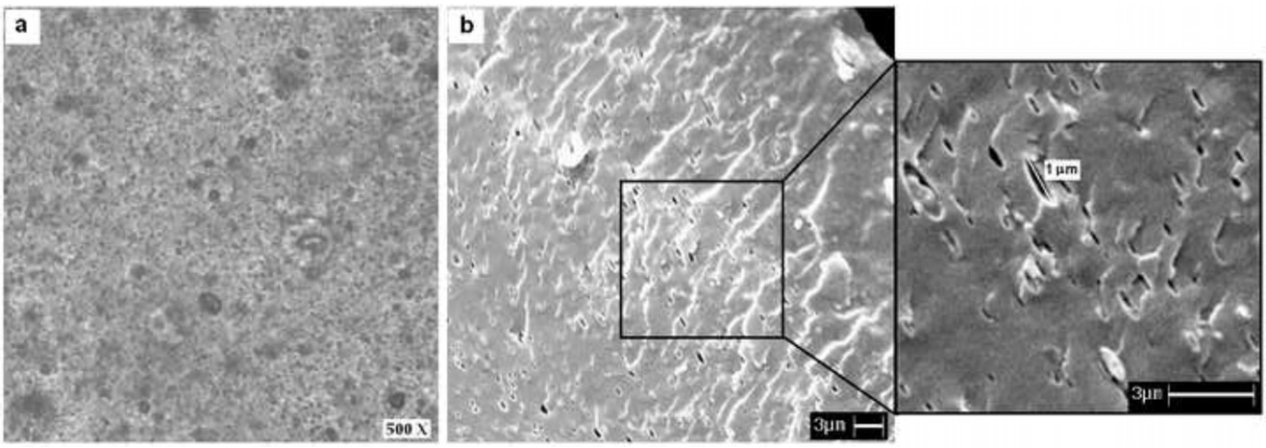

Fig. 2. Light microscopy (a) and scanning electron (b) micrographs of keratin membrane containing 1% w/w CER3 and 1% w/w CER6.

Table 2
Frequencies (cm^{-1}) and assignments of deconvoluted amide I band for human skin and keratin membranes at different compositions.

Assignment	Human epidermis	Membrane				
		1	2	3	4	5
Hys-ring vibration	1596	1594	1595	1595	1595	1595
Ceramides	1611	–	1612*	–	1611	1611
		–		1618	–	1618**
β-sheet intermolecular	1620	1621	1623	1627	1628	1629
β-sheet intramolecular	1633	1632	1631	1631	1634	1635
Random coil	1644–1651	1645–1649	1644–1650	1643–1649	1644–1649	1642–1650
α Helix	1660	1660	1660	1658	1658	1658
Turn	1668	1668	1668	1668	1668	1668
	1676	1674	1675	1674	1675	1674
	1681	1682	1681	1681	1681	1682
	1691	1695	1691	1691	1690	1694

* CER3: The peak is centred at 1613 cm^{-1}.
** CER6: The peak is centred at 1617 cm^{-1}. Two shoulders are present at 1607 and 1632 cm^{-1}.

Table 3
CH_x stretching vibrations (cm^{-1}) and assignments for raw ceramides, human skin and membranes at different compositions.

Assignments	CER3	CER6	Human epidermis	Membrane				
				1	2	3	4	5
Asym CH_3	2955	2956	2956	2957	2957	2957	2958	2959
Asym CH_2	2915	2915	2917	2923	2919	2920	2920	2923
Sym CH_3	2873	2874	2872	2872	2873	2873	2873	2873
Sym CH_2	2849	2849	2850	2855	2851	2851	2851	2853

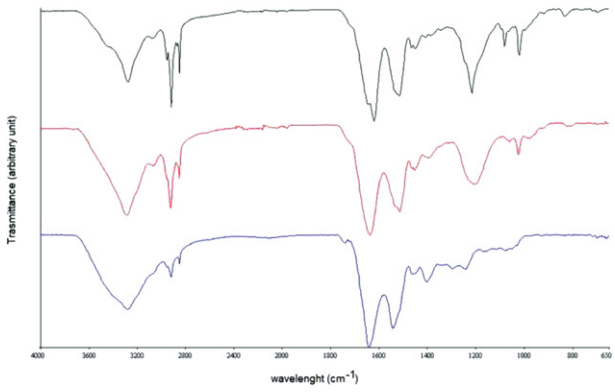

Fig. 3. ATR-FTIR spectra of keratin membranes made of pure keratin (black line) and containing 1% w/w CER3 and 1% w/w CER6 (red line). The spectrum of human epidermis (blue line) is also reported, as reference. (For interpretation of the references to color in this figure legend, the reader is referred to the web version of this article.)

The differences in wavenumber of asymmetric and symmetric stretching vibrations of CH_2 and CH_3 in the spectra of Membranes 2–5 with respect to Membrane 1 (Table 3) were attributed to a modification of the CERs solid state after blending with the regenerated keratin indicating a partial solubilization within the keratin polymeric network. Indeed, during the membranes production, CERs were maintained in suspension, as confirmed by the microscopic analysis of the membranes and the possible rearrangement from the orthorhombic structure toward the hexagonal one was unlikely.

3.2. *In vitro diffusion studies*

The effects of membrane composition and thickness on IB diffusion were reported in Table 1 and the similarity in fluxes values were compared to those of human epidermis from three different donors ($J_1 = 6 \pm 1\ \mu g \times h/cm^2$; $J_2 = 3 \pm 0\ \mu g \times h/cm^2$; $J_3 = 2 \pm 0\ \mu g \times h/cm^2$, [20]) using the factor of difference value, *FoD* [30].

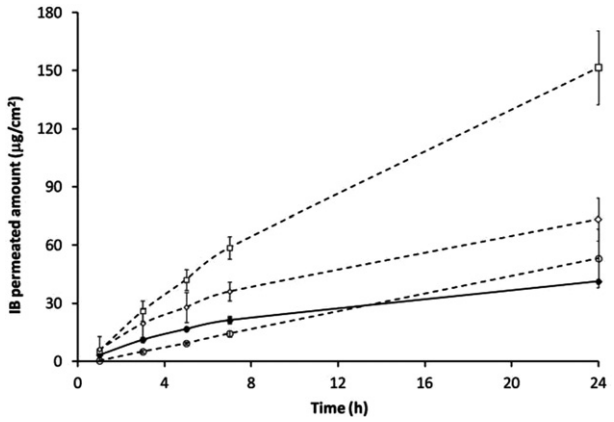

Fig. 4. IB permeation profile through keratin membrane containing 1% w/w CER3 and 1% w/w CER6 (solid line) with respect to human epidermis from three different donors (dashed line).

The *FoD* value was calculated as follows:

$$FoD = \frac{J_m}{J_h}$$

where J_m denotes the flux through the artificial membrane and J_h refers to the flux through human epidermis.

It was suggested that an animal model represents a significant prediction for the human skin behaviour if its associated *FoD* value is less than three [30]; in this set of experiments this value was reduced to the 0.5–1.5 range.

Membranes made only by regenerated keratin showed weak barrier properties and the IB flux was overestimated. Indeed, the flux was twice with respect to human epidermis and this value was significantly higher also according to the Bonferroni–Holm post hoc analysis ($p = 0.002$) with respect to those obtained by human epidermis.

By adding 1% of a single CER in Membranes 2 and 3, the IB flux significantly decreased with respect to the membrane of pure keratin ($p < 0.001$) and the drug permeated amounts were in the same order of magnitude to human epidermis ($p > 0.02$; Table 1). Despite the underestimation, these data confirmed the fundamental role played by CERs in the design of artificial membranes and also that the physical dispersion of these components within the keratin membrane was sufficient to contribute to the reduction of the IB diffusion.

The combination of both CERs at the concentration of 0.5% and 1% w/w improved the IB permeated amount (Table 1). Indeed, the flux of both membranes was statistically different to those containing only a single type of CERs ($p > 0.001$) and comparable to those of human epidermis ($p > 0.56$). Three specimens of Membrane 5 provided reproducible data in terms of amount of permeated drug at each time point and the profiles obtained by human epidermis from three different donors and keratin membranes were superimposable (Fig. 4). Hence, Membrane 5 containing 1% of both CERs was considered worthy of further investigation. In particular, attention was focused on the effect of thickness, namely 60, 140 and 180 μm. As expected the thicker the membrane, the lower the flux (Table 1), as evidenced by the *FoD* trend. Nevertheless, according to the Bonferroni–Holm post hoc analysis, the fluxes were not statistically different to those obtained with human epidermis ($p > 0.08$) or the 180 μm-thick membranes.

Because of the ease of handling, the 180 μm-thick membranes were considered worthy to predict the permeability of IB. Its versatility was further investigated using other two drugs, namely PR and TS. The permeation profiles of PR from both physiological solution and mineral oil were superimposable to those of human epidermis (Fig. 5 a and b) and the *FoD* values were 0.56 and 0.51 for PR in physiological solution and mineral oil, respectively, demonstrating the membrane

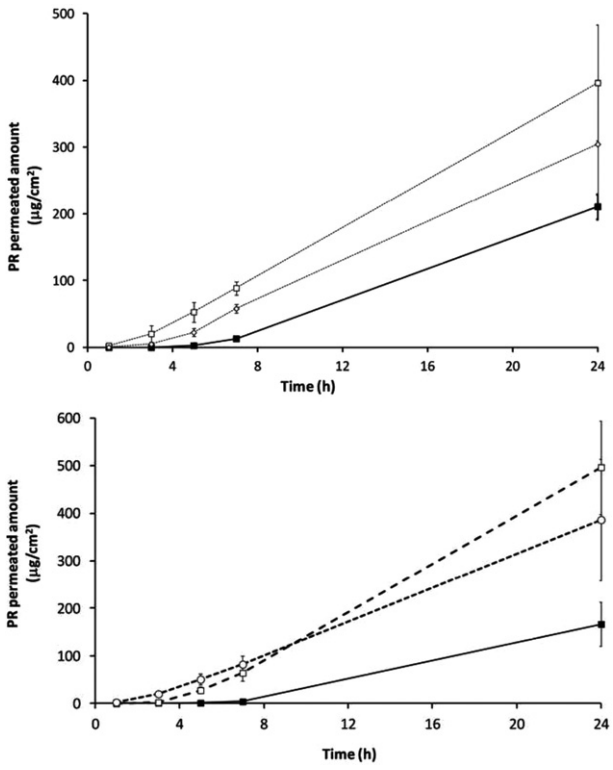

Fig. 5. Permeation profiles of PR from (a) physiological solution and (b) mineral oil through keratin membrane containing 1% w/w CER3 and 1% w/w CER6 (solid line) with respect to human epidermis (dashed line).

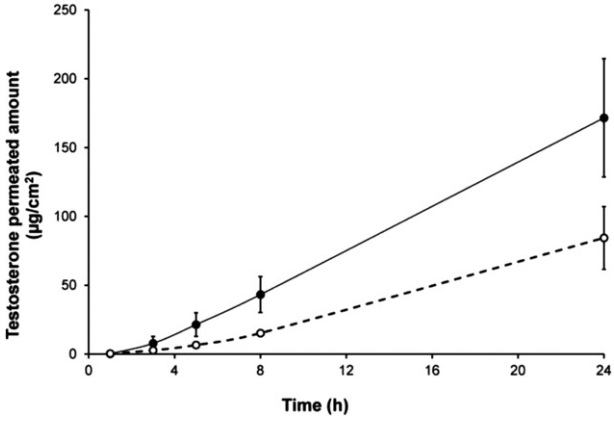

Fig. 6. TS permeation profile through keratin membrane containing 1% w/w CER3 and 1% w/w CER6 (solid line) with respect to human epidermis (dashed line).

resistance in the presence of mineral oil. The only difference was represented by a slight delay in lag time (Fig. 5 a and b).

A different behavior was evidenced in the case of the permeation profile of TS from a water/ethanol solution. In this case, the diffusion patterns through human epidermis and Membrane 5 resulted similarly only in the early data points, namely 5 h (Fig. 6). Afterwards the diffusion of TS increased since Membrane 5 did not maintain its integrity over a prolonged period of time. Indeed, at the end of the permeation experiment the intensity of the main ATR-FTIR bands in Membrane 5 decreased and their wavenumbers slightly shifted. It may be assumed that ethanol affected the biophysical properties of keratin membranes enhancing its fluidity followed by a detrimental effect on its stability. Hence, the current membrane cannot be used when organic solvents are selected as donor phase.

4. Conclusion

The combination of regenerated keratin and CERs permitted the development of simplified membranes of stratum corneum suitable to match the diffusion of small molecules through human epidermis as demonstrated by comparing the diffusion profiles of three model drugs. Nevertheless, the preparation method did not permit the production of membranes stable in presence of organic solvents, such as ethanol, over a prolonged period of time. However, the approach of using regenerated keratin to scaffold the lipid components of stratum corneum can permit the design of membranes with an environment closer to the outermost layer of the epidermis with respect to other proposed systems. As a matter of fact the latter consist of porous substrates (i.e. filters) covered and/or embedded with lipid systems [31,32,12] and therefore cannot take into account possible interactions among the permeant and the protein domain of stratum corneum.

References

[1] OECD. Skin absorption: in vitro method. Test Guideline 428; 2004a.
[2] OECD. Guidance document for the conduct of skin absorption studies number 28. OECD series on testing and assessment; 2004b.
[3] Huong S.P., Bun H., Fourneron J.D., Reynier J.P., Andrieu V. Use of various models for in vitro percutaneous absorption studies of ultraviolet filters. Skin Research and Technology. 2009;15(3):253–261.
[4] Southwell D., Barry B.W., Woodford R. Variations in permeability of human skin within and between specimens. International Journal of Pharmaceutics. 1984;18(3):299–309.
[5] Schaefer U.F., Hansen S., Schneider M., Luengo Contreras J., Lehr C.M. Models for skin absorption and skin toxicity testing. In: drug absorption studies in situ, in vitro and in silico models. Biotechnology: Pharmaceutical Aspects. 2008;VII(1):3–33.
[6] Bronaugh R.L., Stewart R.F., Congdon E.R. Methods for in vitro percutaneous absorption studies. II. Animal models for human skin. Toxicology and Applied Pharmacology. 1982;62:481–488.
[7] Gooris G.S., Bouwstra J.A. Infrared spectroscopic study of stratum corneum model membranes prepared from human ceramides, cholesterol, and fatty acids. Biophysical Journal. 2007;92:2785–2795.
[8] Kirfel J., Magin T.M., Reichelt J. Keratins: a structural scaffold with emerging functions. Cellular and Molecular Life Sciences. 2003;60(1):56–71.
[9] Gu L.H., Coulombe P.A. Keratin function in skin epithelia: a broadening palette with surprising shades. Current Opinion in Cell Biology. 2007;19(1):13–23.
[10] Bouwstra J.A., Goris G.S., van der Spek J.A., Bras W. Structural investigation of human stratum corneum by small angle X-ray scattering. Journal of Investigative Dermatology. 1991;97:1005–1012.
[11] Bouwstra J.A., Goris G.S., Bras W., Dowing D.T. Lipid organization in pig stratum corneum. Journal of Lipid Research. 1995;36:685–695.
[12] Di Nardo A., Wertz P., Giannetti P.A., Seidenari S. Ceramide and cholesterol composition of the skin of patients with atopic dermatitis. Acta Dermato-Venereologica. 1998;78:27–30.
[13] Ishikawa J., Narita H., Kondo N., Hotta M., Takagi Y., Masukawa Y. et al. Changes in the ceramide profile of atopic dermatitis patients. Journal of Investigative Dermatology. 2010;130:2511–2514.
[14] Hoppel L., van der Heijden R., Hankemeier T., Vreeken R.J., Bouwstra J.A., van Smeden J. LC/MS analysis of stratum corneum lipids: ceramide profiling and discovery. Journal ofLipid Research. 2011;52:1211–1221.
[15] de Jager M.W., Gooris G.S., Dolbnya I.P., Ponec M., Bouwstra J.A. Modelling the stratum corneum lipid organisation with synthetic lipid mixtures: the importance of synthetic ceramide composition. Biochimica et Biophysica Acta. 2004;1664(2):132–140.
[16] Groen D., Gooris G.S., Ponec M., Bouwstra J.A. Two new methods for preparing a unique stratum corneum substitute. Biochimica et Biophysica Acta. 2008;1778(10):2421–2429.
[17] Ochalek M., Heissler S., Wohlrab J., Neubert R.H.H. Characterization of lipid model membranes designed for studying impact of ceramide species on drug diffusion and penetration. European Journal of Pharmaceutics and Biopharmaceutics. 2012;81(1):113–120.
[18] Sinko B., Garrigues T.M., Balogh G.T., Nagy Z.K., Tsinman O., Avdeef A. et al. Skin-PAMPA:a new method for fast prediction of skin penetration. European Journal of Pharmaceutical Sciences. 2012;45:698–707.
[19] Cilurzo F., Alberti E., Minghetti P., Gennari C.G.M., Casiraghi A., Montanari L. Effect of drug chirality on the skin permeability of ibuprofen. International Journal of Pharmaceutics. 2010;386(1–2):71–76.
[20] Cilurzo F., Minghetti P., Alberti E., Gennari C.G.M., Pallavicini M., Valoti E. et al. An investigation into the influence of counter-ion on the RS-propranolol and S-propranolol skin permeability. Journal of Pharmaceutical Sciences. 2010;99(3):1217–1224.
[21] Aluigi A., Zoccola M., Vineis C., Tonin C., Ferrero F., Canetti M. Study on the structure and properties of wool keratin regenerated from formic acid. International Journal of Biological Macromolecules. 2007;41:266–273.
[22] Tonin C., Aluigi A., Vineis C., Varesano A., Montarsolo A., Ferrero F. Thermal and structural characterization of poly(ethylene-oxide)/keratin blend films. Journal of Thermal Analysis and Calorimetry. 2007;89:601–608.
[23] Laemmli U.K. Cleavage of structural proteins during the assembly of the head of bacteriophage T4. Nature. 1970;227:680–685.
[24] Savitzky A., Golay J.E. Smoothing and differentiation of data by simplified least squares procedures. Analytical Chemistry. 1964;36:1628–1639.
[25] Van De Sandt J.J.M., Van Burgsteden J.A., Cage S., Carmichael P.L., Dick I., Kenyon S. et al. In vitro predictions of skin absorption of caffeine, testosterone, and benzoic acid: a multi-centre comparison study. Regulatory Toxicology and Pharmacology. 2004;39:271–281.
[26] Cilurzo F., Minghetti P., Casiraghi A., Tosi L., Pagani S., Montanari L. Polymethacrylates as crystallization inhibitors in monolayer transdermal patches containing ibuprofen. European Journal of Pharmaceutics and Biopharmaceutics. 2005;60:61–66.
[27] Netzlaff F., Kaca M., Bock U., Haltner-Ukomadu E., Meiers P., Lehr C.M. et al. Permeability of the reconstructed human epidermis model Episkin® in comparison to various human skin preparations. European Journal of Pharmaceutics and Biopharmaceutics. 2007;66(1):127–134.
[28] Crewther W.G., Fraser R.D.B., Lennox F.G., Lindley H. The chemistry of keratins. Advances in Protein Chemistry. 1965;20:191–346.
[29] Byler D.M., Susi H. Examination of the secondary structure of proteins by deconvolved FTIR spectra. Biopolymer. 1986;25:469–487.
[30] Cilurzo F., Minghetti P., Sinico C. Newborn pig skin as model membrane in in vitro drug permeation studies: a technical note. AAPS PharmSciTech. 2007;8(4):97–100.
[31] de Jager M, Groenink W., Guivernau R.B., Andersson E., Angelova N., Ponec M. et al. A novel in vitro percutaneous penetration model: evaluation of barrier properties with p-aminobenzoic acid and two of its derivatives. Pharmaceutical Research. 2006;23(5):951–960.
[32] de Jager M., Groenink W., van der Spek J., Janmaat C., Gooris G., Ponec M. et al. Preparation and characterization of a stratum corneum substitute for in vitro percutaneous penetration studies. Biochimica et Biophysica Acta. 2006;1758(5):636–644.